Flexural fatigue damage analyses of recycled rubber-modified epoxy-based composites reinforced with alumina fibres

Alaeddin Burak Irez, Emin Bayraktar, Ibrahim Miskioglu

Flexural fatigue damage analyses of recycled rubber-modified epoxy-based composites reinforced with alumina fibres

Alaeddin Burak Irez[1] | Emin Bayraktar[2] | Ibrahim Miskioglu[3]

[1] CentraleSupélec, Université Paris-Saclay, Gif-sur-Yvette, France

[2] School of Mechanical and Manufacturing Engineering, Supmeca-Paris, Saint-Ouen, France

[3] ME-EM Department, Michigan Technological University, Houghton, MI

Correspondence
Emin Bayraktar, School of Mechanical and Manufacturing Engineering, Supmeca-Paris, Saint-Ouen, France.
Email: bayraktar@supmeca.fr

Abstract

Manufacturers have been working towards finding clean and cost-efficient solutions by utilizing recycled materials to produce new components. Recycled rubber is one such material widely used in aeronautic and automotive industries. In this study, fresh scrap ethylene-propylene-diene-monomer (EPDM) rubber is mixed with epoxy to manufacture novel composites with the addition of alumina (Al_2O_3) fibres. These composites can potentially be used to manufacture components subjected to cyclic loading, and to ensure reliability of such components, fatigue behaviour of these composites should be evaluated. This article describes the manufacturing of recycled rubber-modified epoxy-based ternary composites and their fatigue behaviour as well as toughening mechanisms. Dynamic mechanical analysis (DMA) was performed to determine thermomechanical properties. Three-point bending and flexural fatigue tests and Shore D hardness measurements were carried out to determine mechanical properties. After static/fatigue fracture, fracture surfaces were observed with scanning electron microscope (SEM) to determine toughening mechanisms in these composites.

KEYWORDS

alumina fibres, epoxy, flexural fatigue, recycled rubber, SEM

1 | INTRODUCTION

Currently, recycling of materials is attracting considerable attention around the world due to the environmental and economic concerns. Amongst the materials that can be recycled, rubber has a very important place in many industries. At the end of its service life, scrap rubber deposited in landfills causes environmental problems including soil contamination and creating a habitat for mosquitos.[1-3] The impact of the scrap rubber on the environment can be reduced if it is recycled, and one area to utilize the recycled rubber is in the manufacturing of

Nomenclature: AF, Alumina fibre; ASTM, American Society for Testing and Materials; Cl, Confidence level; DMA, Dynamical mechanical analysis; EPDM, Ethylene propylene diene monomer; OM, Optical microscope; PID, Proportional-integral-derivative controller; R, Load ratio during fatigue tests; RMSE, Root mean square error; SDD, Standard deviation; SEM, Scanning electron microscopy; S-N, S, maximum fatigue stress; N, number of fatigue cycles; TLM, Transmission light microscopy; 3PB, Three-point bending tests; α, Weibull shape parameter; $d(N)$, Cumulative damage; E', Storage modulus; E'', Loss modulus; ε_{ave}, Average strain; $\varepsilon_{\min_i}$, Initial minimum strain; ε_n, Instantaneous strain; N_f, Cycle to failure; $P(N)$, Weibull probability of survival; *tan* δ, Mechanical loss angle tangent; u, Weibull scale parameter

novel composites. Composites with recycled rubber as one of its constituents can have some significant advantages compared with existing composite materials. These composites can be suitable for applications where high toughness, high resistance to impact is desirable. In addition to environmental benefits, use of recycled rubber provides an important cost advantage for the manufactured composites.

Depending on the source, scrap rubbers may contain metallic inclusions, fibres, and impurities and may have been subjected to stresses. An example of such a case would be the scrap rubber obtained from ground rubber tires (GTR). The presence of metallic inclusions can cause scrap rubber to oxidize and overheat easily which may lead to self-ignition. The impurities may reduce the affinity of the rubber to bond with the other constituents of the composite. In this study, recycled rubber was procured from a sports equipment manufacturer. It is recovered completely as fresh scrap, and it does not contain any metallic inclusions or fibres and have not been subjected to stresses during its service life. This constitutes the original part of this study.

The matrix material chosen for the composites manufactured was epoxy. Epoxy has relatively low cost, high specific strength, stiffness, and chemical resistance. It is also environmentally stable, easy to process, and does not require the use of an extruder as in the case of polypropylene and polyethylene.[4] However, epoxies due to their highly cross-linked network structure can be brittle. Hard particles such as alumina fibres (AFs) can be incorporated into the matrix to toughen the epoxies.[5,6] In case of a homogeneous distribution, addition of AFs ensures desired mechanical properties due to its favourable structural characteristics such as interlocking effects of fibres.[7-11] In addition, alumina fibres have a very high compressive strength, and it has a greater elastic modulus than carbon fibre in radial direction which provides another advantage to these composites. As a result, low-cost, green, epoxy-based hybrid composites can be manufactured with recycled rubber with the addition of AFs.

Despite the advantages mentioned above, using recycled rubber has some drawbacks. During rubber manufacturing, vulcanization process is carried out to improve the properties of rubber. During vulcanization, free links of rubber are combined with sulphur atoms to form cross-links. However, when the already vulcanized scarp rubber is used in composite manufacturing, it is difficult to create chemical bonding between recycled rubber and epoxy matrix due to the lack of free links. Therefore, lack of chemical bonding leads to some interface problems. In addition, recycled rubber particles tend to agglomerate due to van der Waals forces, and these agglomerations may act as stress concentrators and cause premature failure. Thus, these drawbacks should be considered in the manufacturing process.

Composites containing recycled constituents are generally used in low-cost applications. However, in this study as a novelty, the AFs are added as a reinforcement in an effort to expand the potential applications of this new composite to aeronautic and automotive industries.[12] For instance, in a passenger car, fuel tank mountings and suspension system's auxiliary parts can be manufactured by such a composite. Because of the vibrations induced by engine and road conditions, these components will be subjected to cyclic loading. Hence, fatigue behaviour of these composites should be evaluated to assess the reliability of these structures. Also, to the best of authors' knowledge, fatigue behaviour of the recycled constituent composites has not been examined in detail in the literature.

The evaluation of the fatigue behaviour of the composites can be done numerically or experimentally. Some researchers performed numerical studies that can be classified into three major categories as fatigue life models, phenomenological models, and progressive damage models.[13,14] Amongst these models, progressive damage model is considered as the most advanced and consistent model. Because, it can predict the fatigue life time along with the degradation of the material properties in the composite specimen by exploiting different damage mechanisms. In addition, fatigue crack growth under variable amplitude cyclic loading (VACL) is frequently observed in engineering applications, yet the modelling is quite complex. The application of classical Paris law to predict the fatigue life under VACL may lead to considerable error. The other models also have shortcomings in prediction of fatigue life under VACL.[15]

Numerical modelling of the composites manufactured in this study presents some challenges. First, the microstructure of recycled rubber-modified composites is particularly complicated. It exhibits intensive inhomogeneity and anisotropy, which brings notable difficulties in the prediction of fatigue properties and damage mechanism analysis. For instance, using unit cell homogenization in the modelling does not reflect the real microstructure of the material. Therefore, some significant discrepancies between modelling and experimental results can be observed. Second, irregular shapes of the recycled rubber can cause difficulties in modelling while assigning interparticle interactions and grain boundaries. These challenges in modelling may lead to significant deviations from the experimental results. Therefore, in this study, for reliable results, it is decided to perform fatigue tests only.[16-18]

This work presents a low-cost manufacturing process of recycled rubber in epoxy matrix reinforced with alumina fibres to create novel composites. The main objective of this research is to evaluate the fatigue behaviour of these composites as well as to determine their mechanical and thermomechanical properties. During this study, thermomechanical properties such as glass transition temperature were determined with dynamical mechanical analysis (DMA). Surface hardness of the composites was measured by a Shore D hardness tester. Then, quasistatic three-point bending (3 PB) tests were performed with rectangular specimens. Fatigue tests under flexural loading were carried out to determine the stress-life curves (S-N). After mechanical tests, fracture surfaces were observed by means of scanning electron microscopy (SEM) to study the toughening and damage mechanisms.

2 | EXPERIMENTAL PROCEDURE

2.1 | Material processing

Epoxy-based composites used in this study were prepared by solution blending procedure. At first, Bisphenol A-type Huntsman Araldite DBF epoxy resin was heated to 65°C in order to decrease its viscosity. Then, alumina fibres obtained from Merck Chemicals were added to epoxy resin per weight percentages given in Table 1. This blend was mixed with a high-speed shear mixer for 1 hour at 65°C to homogenize the mixture. Next, the recycled EPDM rubber was gradually added to this mixture, and the blend was mixed for two more hours at 65°C to prevent the agglomerations. Following high shear stirring, the blend was sonicated for 30 minutes to improve its homogeneity, and the mixture was cooled down to room temperature to add the hardener. Adding the hardener at high temperatures causes rapid solidification, which in turn may lead to inhomogeneous cross-linking reaction in some regions of the composite. As a result, variation in material properties, depending on the solidified areas, can be observed in the manufactured composite. After the mixture cooled down to room temperature, 20 wt% hardener (Aradur HY-956 Huntsman) based on the epoxy content was added, and this final compound was mixed for 15 minutes. Then, the mixture was poured into silicon moulds and placed in a vacuum chamber at room temperature for degassing for 20 minutes. Afterwards, moulds were left at room temperature for 24 hours to complete the curing. This composite manufacturing process is illustrated in Figure 1.

In this study, wettability of alumina fibres in the epoxy matrix plays an important role in the material properties of the resulting composite. In the literature,

TABLE 1 Composition of recycled rubber-modified epoxy-based composites reinforced with AFs

LRAL Composites	Alumina Fibre Content, wt%			
Rubber Content, wt%	0%	5%	7.50%	10%
20%	LR20	LR2AL5	LR2AL7.5	LR2AL10
30%	LR30	LR3AL5	LR3AL7.5	LR3AL10

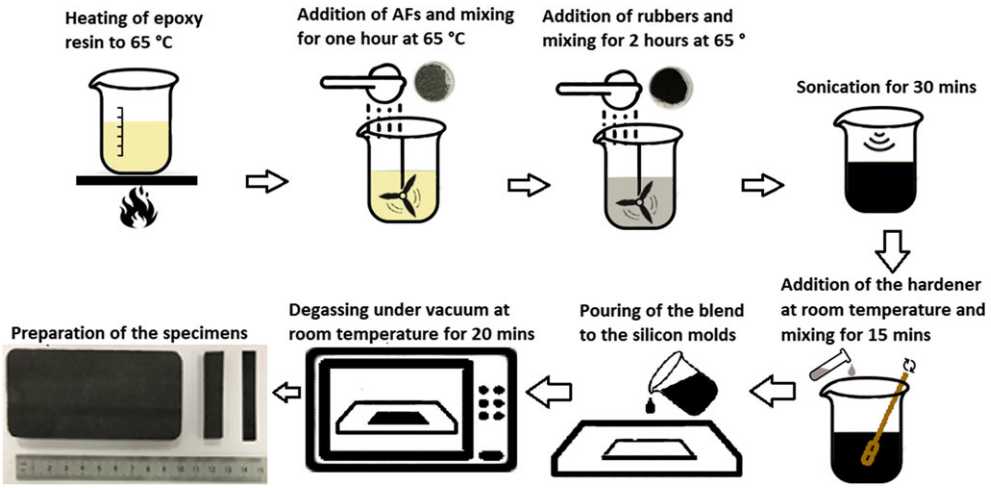

FIGURE 1 Manufacturing steps of liquid epoxy-based recycled EPDM-modified composites [Colour figure can be viewed at wileyonlinelibrary.com]

there are some methods to improve the wettability of the fibres with polymer matrices including polypropylene-g-maleic anhydride (PP-g-MA) treatment of the fibres, etching of the surface of fibres with a hydrochloric acid and sodium hydroxide, or treatment of the fibres by a silane coupling agent. Low-temperature oxygen plasma treatment is also used by various researchers to improve wettability of the fibres. After the fibres processed for improved wettability are used in the composite, contact angle measurement is carried out to see the efficiency of these methods. However, during the literature review of this study, it has been observed that alumina fibres have a good wettability with epoxy resin. After manufacturing of the composite, a polished cross section was cleanly fractured, and a decent bonding of the fibres to epoxy was observed.[19] For this reason, surface treatment of fibres was not implemented in order not to degrade the cost-effectiveness of the composites in consideration.

In this study, different contents of rubber and AFs are used to study their effects on mechanical properties. In Table 1, detailed compositions of AFs and rubber-modified epoxy composites (called as LRAL composites hereafter) are given.

2.2 | Material characterization and microscopical observation

Surface hardness measurements of the specimens were performed after curing. Shore D hardness test measurements on the polished flat surfaces of the specimens were carried out according to ASTM D 2240 using a Shore D hardness tester (type HBD-100-0).

Dynamic properties, storage modulus (E'), loss modulus (E''), and mechanical loss angle tangent ($tan\ \delta$) of the epoxy-based composites were investigated using a dynamic mechanical analyser Q800 system by TA Instruments. Single cantilever bending mode was used, and data were collected at a frequency of 1 Hz, 0.1% strain in the temperature range from 20°C to 130°C. The samples were 10 mm wide, 50 mm long, and 3 mm thick.

Quasistatic three-point bending tests (3PB) were carried out according to the ASTM D790. An Instron 5569 testing system was used for these tests. Deflection of the specimen was measured by the crosshead position, and crosshead speed was selected as 1 mm/minute. Flexural strength, elasticity modulus in bending (flexural modulus), and strain were obtained from the test results. The test specimen was placed in the bending fixture of the universal testing machine and loaded until it fractured. At least five specimens for each composition were used, and average values of the results were given together with standard deviations.

Fatigue tests were realized with MTS 810 hydraulic fatigue testing machine in flexural mode. During fatigue tests load ratio (R) was selected 0.1. Tests were carried out at room temperature in the force-control mode. PID controller of the test machine was adjusted prior to tests for each different composition group to have reliable test results. At least two specimens were used for each stress level to ensure repeatable results. After conducting the tests, S-N curves were plotted to determine the fatigue time of these composites.

Fracture surface damage analyses and microstructural observations were realized by means of an optical microscope (OM) and a scanning electron microscope (SEM). SEM observation was performed on fracture surface of the tested specimens with Scope/JSM-6010LA Jeol electron microscope.

3 | RESULTS AND DISCUSSIONS

3.1 | Surface hardness and the microstructure of the composites

Surface hardness of the composites was measured by a durometer using Shore D scale. Hardness is important for the potential applications of the manufactured composites. At least five measurements were taken from different points on the surface, and average values and the standard deviations are given in Table 2.

It can be observed that addition of 5 wt% AF did increase the hardness of the composite. However, there was no significant change in hardness when AF content was increased further to 7.5 and 10 wt%. The increase in the standard deviations can be attributed to the increase in the heterogeneity of the composites with the increased wt% of the constituents.

An example for the microstructure of the composites is given in Figure 2A and 2B. In Figure 2A and 2B, a sectioned specimen was used to observe the microstructure of the AF-reinforced hybrid composites by means of SEM and transmitted light microscope (TLM). White particles in Figure 2A indicate alumina particles whereas black particles in Figure 2B show recycled rubber.

TABLE 2 Shore D hardness of the manufactured composites

Composition Name	Shore D	Composition Name	Shore D
LR20	72.8 ± 0.2	LR30	64.4 ± 0.3
LR2AL5	75.4 ± 0.5	LR3AL5	69.8 ± 0.5
LR2AL7.5	76.8 ± 0.6	LR3AL7.5	67.2 ± 1.1
LR2AL10	75.2 ± 1.2	LR3AL10	70.0 ± 0.8

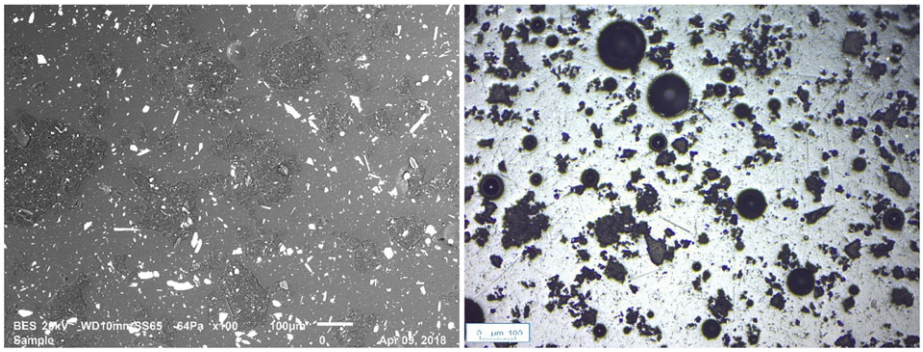

FIGURE 2 Microstructural observation of LR2AL10 with (A) SEM and (B) transmitted light microscope (TLM) [Colour figure can be viewed at wileyonlinelibrary.com]

Different size rubber particles (10-70 μm) can also be observed in Figure 2B. Figure 2A shows that different length AFs are present in the composite.

3.2 | Dynamic mechanical analysis of the composites

Thermomechanical characteristics of the composites were investigated by DMA. Fundamental idea on elastic response and viscous response of the material was obtained, respectively, from storage modulus (E') and loss modulus (E'') under dynamic loading. Then, the loss factor ($tan\ \delta$) was determined as the ratio of loss modulus to storage modulus which is a measure of the energy lost from the material under loading.[20] After acquiring the results, T_g can be determined by taking the first inflection point, or the onset of the drop-in storage modulus. However, the simplest approach to determine T_g is taking the peak of $tan\ \delta$.[21]

DMA analysis is important for the manufactured composites. The glass transition temperature can be thought as a temperature limit for the structural applications because mechanical resistance of these composites reduces drastically after T_g and this should be considered during design process. Besides, the effect of reinforcing agents on motion capability of polymer chains manifests itself in the changes of E' and E''. For this reason, DMA analysis is considered as a useful tool to understand the root causes of the thermomechanical behaviour.

The effect of AF content on the thermomechanical properties were examined with the specimens having different AF content but having constant rubber content. DMA analyses were carried out between −60°C and 180°C. The evolution of the storage modulus and $tan\ \delta$ for LR2AL and LR3AL group composites is shown in Figures 3 and 4, respectively. For each composition group, no significant change in the trend of the storage modulus and $tan\ \delta$ curves was observed for negative temperatures as well as temperatures greater than 130°C; hence, the curves in these figures are truncated for low as well as high temperatures.

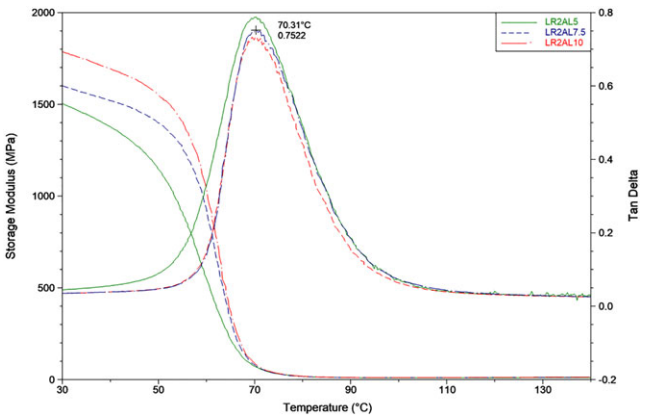

FIGURE 3 DMA curves for the LR2AL group composites [Colour figure can be viewed at wileyonlinelibrary.com]

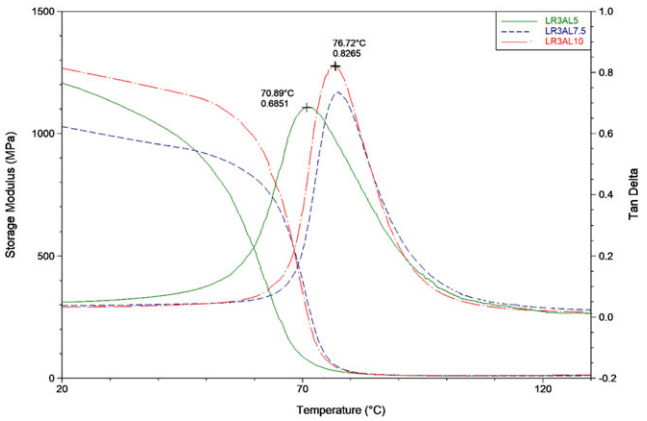

FIGURE 4 Evolution of E' and $tan\ \delta$ as a function of temperature for LR3AL composites [Colour figure can be viewed at wileyonlinelibrary.com]

In Figure 3, it can be observed that increase in the alumina fibre content increased energy storing capability of the composites containing 20 wt% rubber and decreased the peak of the *tan δ* curve. Since the magnitude of *tan δ* is proportional to the internal damping, increase in the alumina fibre content decreased the internal damping. Because, when the number of the fibres is increased, free matrix volume around each fibre decreases and this leads to low matrix mobility. Decrease in polymer chain mobility causes the material to be less deformable, which in turn lowers the internal damping. Also, the storage modulus (E') curves in Figures 3 and 4 show the less deformable nature of the manufactured composites. Increasing fibre content leads to a more rigid composite (higher E').[22,23]

Figure 4 shows that storage modulus of the LR3AL composites was improved also with the increase in alumina fibre content. However, tan δ (implicitly loss modulus) did not exhibit a response similar to LR2AL group. This means that the lost energy is more dependent on the change in the rubber content. In addition, T_g of the LR3AL composites was higher with respect to the LR2AL composites, ie, T_g increased with the increase in rubber content. It can be assumed that increase in the number of the rubber particles in the matrix restricts the motion of the epoxy chains, which leads to the increase in T_g. Also, some functional groups of rubber may react with epoxy, and they can create hydrogen bonding. This bonding can constrain epoxy chain mobility which again can lead to the increase in T_g.[24]

3.3 | Mechanical characterization of the composites

Mechanical properties were examined by 3PB tests, and results are given in Table 3.

TABLE 3 Three-point bending test results of the manufactured composites

Composition Name	Ultimate Flexural Strength, MPa	Flexural Modulus, MPa	Strain at Break
LR20	48.33 ± 1.02	1149.64 ± 20.74	0.045 ± 0.001
LR2AL5	40.17 ± 0.93	1220.77 ± 38.43	0.035 ± 0.001
LR2AL7.5	40.06 ± 1.20	1143.54 ± 42.3	0.043 ± 0.006
LR2AL10	40.65 ± 0.91	1302.47 ± 83.23	0.034 ± 0.001
LR30	34.27 ± 3.77	478.25 ± 64.13	0.037 ± 0.001
LR3AL5	30.61 ± 0.99	962.94 ± 14.23	0.033 ± 0.001
LR3AL7.5	29.59 ± 1.30	1029.57 ± 30.09	0.030 ± 0.001
LR3AL10	39.75 ± 0.60	1259.82 ± 13.64	0.033 ± 0.001

The first inference from Table 3 is that increasing content of rubber results in a decrease on strength of the composites. Moreover, increasing rubber content decreases the strain at break. This trend can be associated with poor interfacial adhesion of the epoxy and EPDM blends. As previously mentioned, due to the former vulcanization process, waste EPDM rubbers do not have any free links on their surface. Therefore, it is difficult to have a chemical bond between epoxy and scrap rubber. Due to the low compatibility between epoxy and waste EPDM, gaps can be observed at the interfaces, and this leads to low stress transfer from the matrix to the rubber particles resulting in reduced overall rigidity of the compounds. In addition, voids can be formed in the epoxy-rubber interface during the solidification because of the different contractions of rubber and epoxy. As a conclusion, when these composites are subjected to loading, these voids constitute the weak points of the composite and cracks can propagate easily along these weak grain boundaries. This situation leads to premature failure. The decrease in the mechanical properties is also related to the low rigidity of waste EPDM. Lastly, the decrease in the mechanical properties can be attributed to limited chain mobility of waste EPDM particles due to their cross-linked nature. In order to support these arguments, in Figure 5A and 5B, fracture surfaces resulting from 3PB tests of compositions with 20 and 30 wt% rubber contents are shown. In Figure 5B, composite with 30 wt% rubber content has more discontinuities as shown with the red arrows and circles at the epoxy and rubber interfaces compared with the composite with 20 wt% rubber content. In these figures, smooth parts indicate epoxy matrix, while rough parts show recycled rubber. Also, in Figure 5 B, rubber particles are seen more in clusters compared with composite with lower rubber content. Hence, because of the reasons stated above, the increase in rubber content increases the number of the discontinuities which leads to the decrease of the strength and strain of the manufactured composites. In order to compensate these negative effects of the recycled rubber, alumina fibres were added to the composite system. The rigid nature of the alumina fibres improved the elasticity modulus of the composites. However, possible detrimental effects of recycled rubbers in stress and strain at break cannot be compensated effectively by AFs.[25,26]

3.4 | Fatigue behaviour of the composites

The data obtained in the fatigue testing were used to plot the Wöhler (S-N) curves to determine the effect of rubber and AF on the fatigue life of the manufactured composites. The S-N curves for all the composites are presented

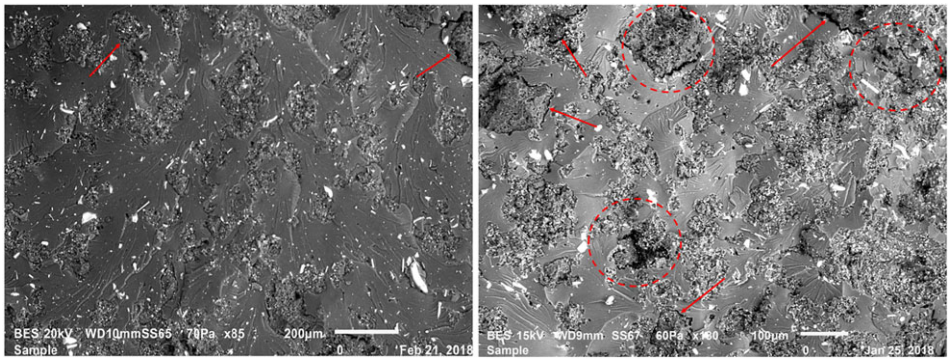

FIGURE 5 Fracture surfaces of waste EPDM-modified epoxy-based ternary composites (A) 20 wt% and (B) 30 wt% of rubber **(NEW FIGURE)** [Colour figure can be viewed at wileyonlinelibrary.com]

in Figure 6. It is observed that AFs are significantly enhancing the fatigue life of the composites compared with those without AFs. Moreover, within LR2AL group, increasing AF content slightly enhances the fatigue life of the composites. On the other hand, the increase in the rubber content results in a considerable decline in the fatigue life of same weight fraction AF-containing composites. This is similar to the trend observed in the 3PB test results. Decrease in flexural strength with the increase in rubber content manifests itself in the decreased fatigue strength of the composites. Root mean square error (RMSE) and standard deviation (SDD) of the residuals of the fitted lines in Figure 6 are presented in Table 4.

Composite fatigue life is affected by the properties of the constituents such as fibre strength, matrix toughness, or the mass fraction of fibres. Using robust fillers such as AFs increased the fatigue life of the composites. The analysis of the distribution of fatigue life can be examined by using Weibull's statistics, for a prescribed confidence

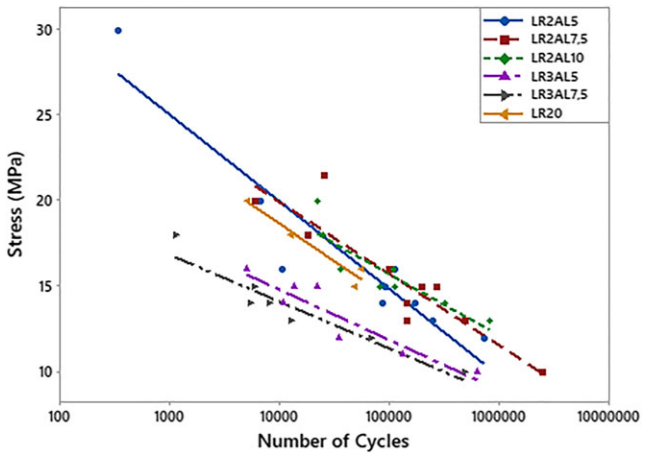

FIGURE 6 S-N curves of the different content recycled rubber and alumina fibre containing composites [Colour figure can be viewed at wileyonlinelibrary.com]

TABLE 4 Residual of fitted lines in S-N curves and Weibull distribution analysis parameters

Composition Name	RMSE ± SDD, MPa	Shape Parameter (α)	Scale Parameter (u)
LR20	0.459 ± 0.530	1.2799	33 490
LR2AL5	1.856 ± 1.984	0.6243	118 855
LR2AL7.5	1.375 ± 1.450	0.6327	259 670
LR2AL10	0.964 ± 1.031	0.8306	170 417
LR3AL5	0.792 ± 0.938	0.6101	76 155
LR3AL7.5	0.717 ± 0.775	0.5121	37 420

level.[27] Weibull analysis suggests a realistic distribution of the fatigue life as a function of stress level with respect to the experimentally obtained values. The probability of survival, $P(N)$, at a number of cycles N under a given load is presented in Equation 1:

$$P(N) = \exp\left[-\left(\frac{N}{u}\right)^{\alpha}\right] \quad (1)$$

where u is the scale and α is the shape parameter of Weibull distribution. Shape parameter (α) is the slope of the Weibull function, and scale parameter (u) is an indicator of the scatter in the data. Fatigue life distribution of each composite group was examined using Weibull distribution function at a 95% confidence level (Cl). The resulting shape and scale parameters are also given in Table 4.

As can be observed in Table 4, AF-reinforced composites have lower shape parameters compared with LR20 group. This means that greater variability in the fatigue cycles is observed in the ternary composites. Moreover, reliability of the results is increasing for $\alpha < 1$.

Another observation, yet an expected one, is that alumina fibres do help to preserve the stiffness of the composite under cyclic loading when compared with the

composites with just rubber added. This conclusion was derived from the comparison of the composite strain over a finite time interval under the same stress level. In each fatigue test, the load was cycled between a minimum and a maximum depending on the preselected load ratio (R). These applied loads lead to a minimum strain (ε_{min}) and a maximum strain (ε_{max}). These strains were determined from the displacement values recorded for each cycle. After the start of the test, when the prescribed load ratio stabilized, a reference minimum strain ($\varepsilon_{\min_i}$) was selected to quantify the evolution of the strain. The ratio of the reference minimum strain ($\varepsilon_{\min_i}$) to instantaneous strain (ε_n) for each cycle was determined. This ratio was accepted as an indicator for the stiffness. In Figure 7, the ratio of ($\varepsilon_{\min_i}$) to (ε_n) is plotted for LR20 (blue curve) and LR2AL5 (black curve) compositions. It is seen that composite with alumina fibre content maintains its stiffness better than only rubber-modified composite. Also, amongst the composites demonstrated in Figure 7, LR20 failed at 48 850th cycle whereas LR2AL5 failed at 91 169th cycle. For LR20 specimen, the complete failure occurred when it lost about 62% of its initial stiffness, whereas for LR2AL5, failure occurred when it lost about 42% of its initial stiffness. The percent of stiffness reduction at failure was not constant, and it changed depending on the material type and the loading level used. However, the general trend between LR and LRAL groups was maintained.

As stated by different researchers, when a composite is exposed to cyclic loading, generally three distinct stages are observed in its stiffness degradation.[28,29] In Figure 7, the first stage is between 0 and 5000 cycles; a relatively high percentage of stiffness degradation is observed probably due to the manufacturing defects such as porosities and agglomerations. After this stage, a slow progressive stiffness decrease occurs over most of the fatigue life of the composite. In the third stage corresponding the last 3000 cycles, more significant damage inside the material takes place, and this results in the total material failure.[30]

The evolution of the stiffness during the fatigue cycles was supported by another term called dynamic secant modulus. Dynamic secant modulus is defined as the slope of each hysteresis loop. This term also is an indicator of the damage evolution of the specimen.[31,32] A comparison of the dynamic secant modulus is presented in Figure 8 for composites with different rubber and AF content tested at the same stress level. In Figure 8, the number of cycles was normalized by cycle to failure (N_f). Figure 8 shows that the presence of AFs leads to higher dynamic secant modulus, which is consistent with elasticity modulus obtained from 3PB tests (E_{LR20} = 1149 MPa, E_{LR2AL5} = 1220 MPa, E_{LR3AL5} = 962 MPa). On the other hand, dynamic secant modulus of LR2AL5 decreased to about 60% of its initial value (from 1360 to 800 MPa) just before failure, and LR3AL5 lost about 35% of its initial secant modulus (from 1050 to 675 MPa) just before failure cycle. This can be attributed to the abundance of particles in the matrix which restricts the mobility of the polymer chains resulting in low deformation of the composite when the rubber content was increased from 20 to 30 wt%.

A practical approach for the damage evolution is introduced by cumulative damage defined as the change in the strain during fatigue loading. Even though this approach gives a relatively rough estimate considering

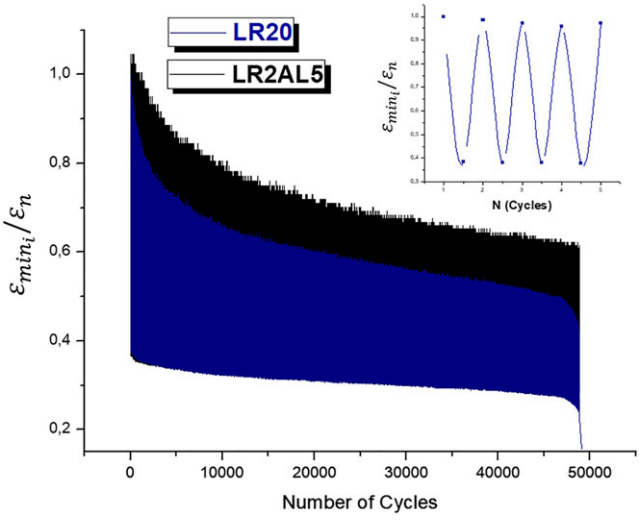

FIGURE 7 Comparison of the stiffness evolution for LR2AL5 and LR20 composites [Colour figure can be viewed at wileyonlinelibrary.com]

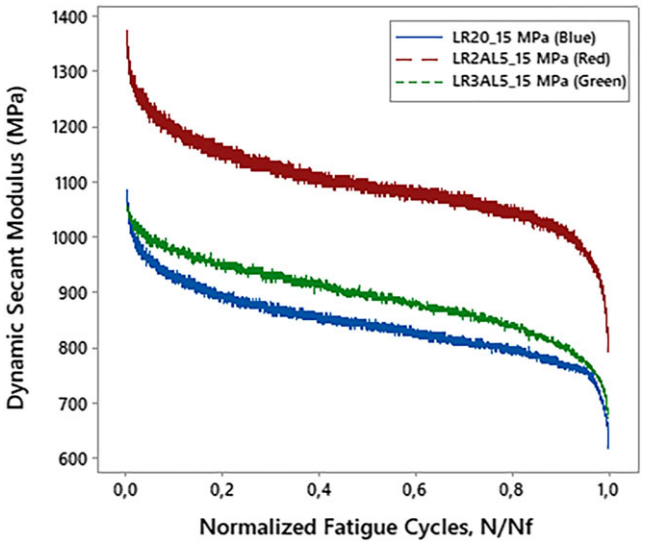

FIGURE 8 Comparison of dynamic secant modulus as a function of number of cycles [Colour figure can be viewed at wileyonlinelibrary.com]

the complexity of the damage mechanisms within composite materials, it enables us to compare macroscopic damage amongst different compositions during the test.[33] In general, cumulative damage is based on the decrease in rigidity during a fatigue test.[34,35] In order to define the cumulative damage, first step is to calculate the average strain (ε_{ave}) for a fatigue cycle as $\varepsilon_{ave} = (\varepsilon_{max} + \varepsilon_{min})/2$. Then, the cumulative damage ($d(N)$) during fatigue loading is calculated by Equation 2:

$$d(N) = \frac{\varepsilon_{ave}(N) - \varepsilon_{ave}(0)}{\varepsilon_{ave}(N_f) - \varepsilon_{ave}(0)} \quad (2)$$

where $\varepsilon_{ave}(0)$ and $\varepsilon_{ave}(N_f)$ are the initial and final average strains, respectively. This expression gives cumulative damage varying between 0 and 1. From this definition, it is possible to compare the influence of rubber and AF contents on $d(N)$ for different compositions as presented in Figure 9.

In Figure 9, it can be observed that for the same stress level of fatigue loading (σ = 15 MPa), increase in rubber content for a constant AF percentage increases the cumulative damage very rapidly. After the relatively slow evolution zone, the curve of $d(N)$ has a steep slope which indicates the rapid progression of the damage leading to final failure. Also, by comparison of the cumulative damage of LR20 and LR2AL5 in the middle of their fatigue life (24 517th cycle and 45 595th cycle, respectively), it is found that $d(N)_{LR20} = 0.436$ and $d(N)_{LR2AL5} = 0.384$. This indicates the positive retardation effect of AFs on cumulative damage of the composites.

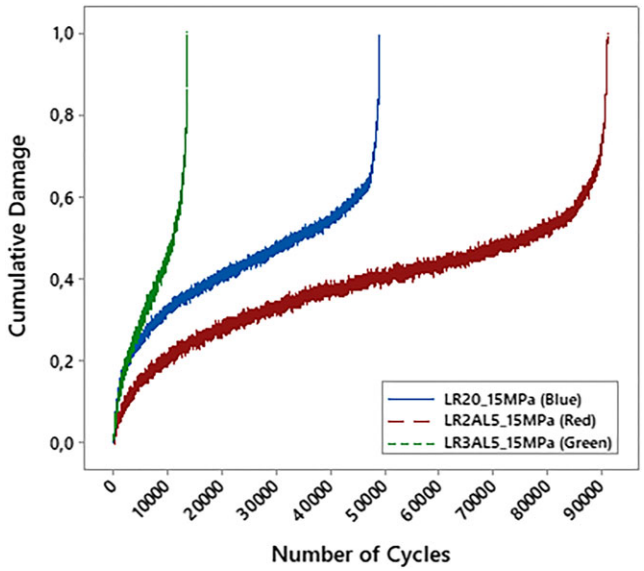

FIGURE 9 Cumulative damage comparison of the composites under same stress level (15 MPa) [Colour figure can be viewed at wileyonlinelibrary.com]

3.5 | Fracture surface observation by means of scanning electron microscopy

Fracture surfaces of the failed specimens from 3PB and fatigue tests were examined with SEM. In Figure 10, many fibres with different dimensions are observed and marked with red arrows and circles on the fracture surface after a 3PB test. The fibres which are aligned near normal to the crack opening or the fracture surface plane play more likely a bridge role. This means that at each bridging site, the fibre generates a discrete traction that lowers the stress applied at the crack tip whereby increasing the fracture toughness. Also, according to another definition, fibre bridging can obstruct crack opening in the crack propagation zone. For instance, to advance the crack, more strain energy should be applied and subsequently dissipated to overcome the constraint in the form of fibre bridging. Resistance to the crack opening is thus improved because of the occurrence of fibre bridging which enhances the fracture toughness.[36-38]

In Figure 11A, some of the attached fibres on the fracture surface after the 3PB test (marked with red arrow) reveal an important length out of the fracture zone, and the majority of them were oriented at an angle to the crack propagation direction (the crack propagation direction is shown with the yellow arrow). This indicates that these fibres were pulled out during the crack propagation. This is an important damage mechanism known as fibre pull-out.

Furthermore, in Figure 11A, it is inferred that when the fibres are aligned at large angles to the crack propagation direction, their embedded length is playing an important role in the fracture mechanism. If a long length of the fibres remains inside the fracture surface, the fibres break. On the other hand, if the embedded

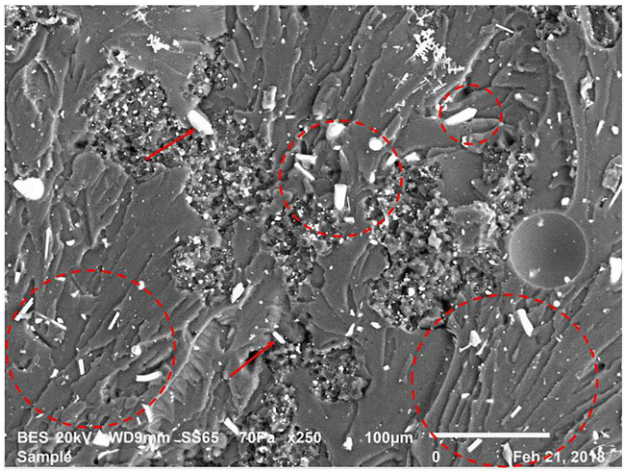

FIGURE 10 Fibre bridging in LRAL group composites **(FIGURE CHANGED)** [Colour figure can be viewed at wileyonlinelibrary.com]

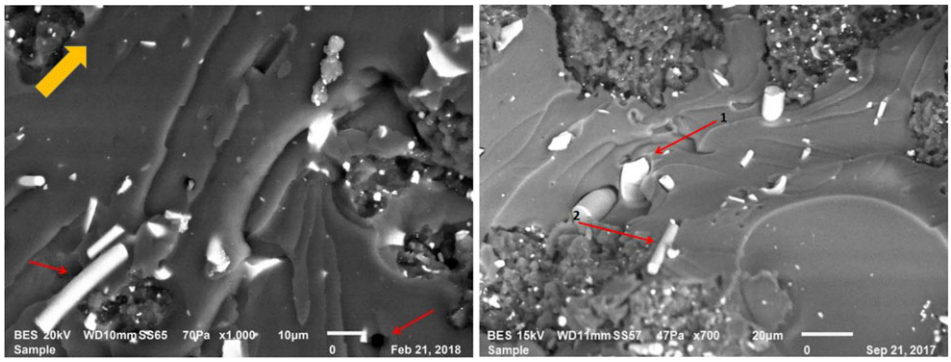

FIGURE 11 Pull-out of the fibres in LRAL group composites [Colour figure can be viewed at wileyonlinelibrary.com]

length of the fibre (variable between 5 and 20 μm) is very short, the fibre tends to be pulled out. If this embedded length falls to an intermediate value, a combined mechanism of fibre breakage and fibre pull-out is observed as shown in Figure 11B.[39,40] In fact, fracture resistance of the materials mainly originates from the work done during the rupture of the matrix and fibres in the path of planar crack. However, a certain amount of work is also spent on pulling out the fibres, which brings additional toughening to the material as experienced in AF-reinforced composites.[41]

According to Figure 11B, the fibre labelled as 1 is broken. As a consequence of strong interface with the matrix, fibres do not pull out easily. Instead, they try to bridge the fracture surfaces. However, if the local stress exceeds the strength of the fibre, it breaks. This condition retards the failure of the material, and it is considered as a toughening mechanism. Also, in the same figure, another fibre labelled as 2 has a poor interface with the matrix.

In relation to the effect of the rubber, in Figure 12A and 12B, shear yielding and diffusion bonding mechanisms are clearly observed on a fatigue fracture surface. Shear yielding is a considerable factor that improves the strength of the polymer in the absence of brittle fracture.[42] Even if the final composite shows a brittle fracture, crack propagation involves a localized plastic and viscoelastic energy dissipating process around the crack tip due to the polymer matrix. As a consequence, this mechanism contributes to energy absorption in the material and improves the fracture toughness of the material.[43]

Lastly, void growth and cavitated rubber particles are seen on the fatigue fracture surfaces as demonstrated in Figure 13A and 13B. Many factors may cause void formation such as curing pressure, resin system, and environmental conditions. Therefore, it is quite difficult to obtain a composite section without any voids. However, when the static and fatigue fracture surfaces were compared, it is found that fatigue fracture surfaces have many more voids in comparison to the static ones. In the epoxy matrix, debonding of the fillers and the plastic deformation of the polymer can significantly influence the number and the size of the voids formed. In this study, AF and recycled EPDM rubber were used to modify the epoxy matrix. Recycled rubber and AFs possess high bulk moduli ($K = E / 3(1 - 2\nu)$). Because, Poisson ratio (ν) of recycled EPDM rubber is around 0.48, also alumina fibres have a high elastic modulus ($E \cong 240$ GPa). This indicates that AFs and waste EPDM particles are very rigid elastic

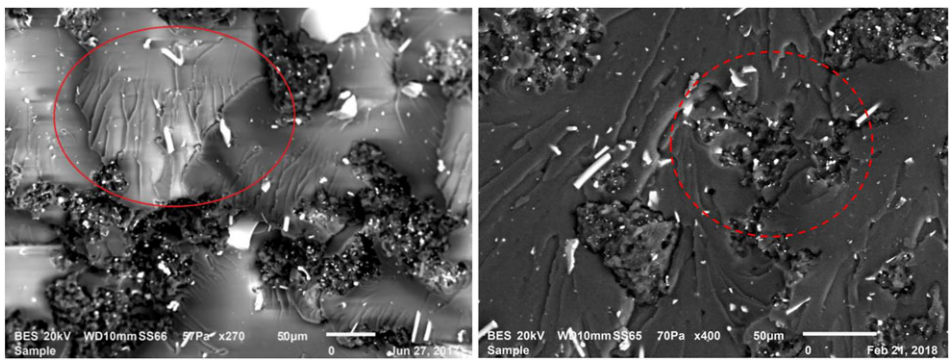

FIGURE 12 (A) Shear yielding and (B) diffusion bonding toughening mechanisms in LRAL group composites [Colour figure can be viewed at wileyonlinelibrary.com]

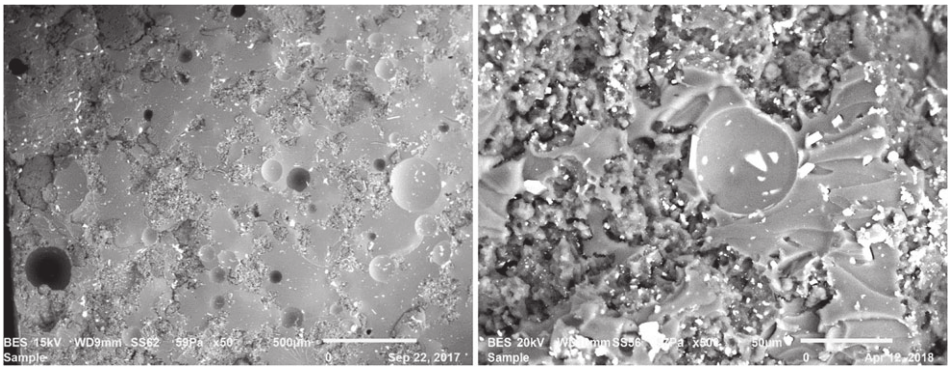

(A) (B)

FIGURE 13 Fatigue fracture surfaces of LR2AL10 group composites

bodies when subjected to triaxial stresses, and they will be eminently resistant to any volumetric deformation. On the other hand, the epoxy matrix has a significantly lower Poisson ratio which is around 0.33. In addition, the epoxy matrix strain softens after yielding, which is a generally observed phenomenon for glassy polymers, and for this reason, the yielded epoxy will be comparably compliant and will deform plastically more easily. However, the "rigid" rubbery phase and AFs will hinder any substantial plastic dilatation in the matrix, unless these rubber particles and AFs debond from the epoxy matrix or if the rubber particles do not internally cavitate. By the interfacial debonding of AFs and rubber, some of the stored strain energy is dissipated, and it is followed by shear band formation and shear yielding of the epoxy matrix surrounding the fillers. Subsequent to debonding and shear yielding, voids originate and grow because of the localized plastic flow of the epoxy matrix next to AFs and rubbers. Then, again some stored strain energy is dissipated by the void growth mechanism including plastic deformation of the epoxy. In static loading, void formation can also occur. However, in cyclic loading, the repetitive nature of the loading increases the density of the voids in the fracture surface.[38,44,45]

The matrix surrounding the voids exhibits a notable plastic deformation as evidenced by the bevelled edges of the voids.[46,47] Furthermore, if the particle-to-particle distance decreases due to the increasing amount of fillers, plastic deformation grows, which may enlarge the size of the voids.[48] Also, cavitated rubber particles seen in Figure 13B produce enhanced shear deformation and lower the crack propagation rates, which improves fatigue life.

4 | CONCLUSION

The new composites were manufactured by the solution blending method. This method is practical to apply. However, viscous characteristics of epoxy require a good mixing process. DMA results indicated that reinforcements may have some different effects on polymer chain mobility. Because of the former vulcanization process, waste EPDM rubber does not have any free links on their surface and this leads to low interface quality between epoxy and waste rubber. Therefore, when these composites are subjected to loading, this interface constitutes the weak points of the composite and cracks can form and propagate easily in the microstructure. As a consequence, premature failure can be observed in composites with high rubber content.

In order to compensate these undesirable effects of rubbers, addition of AFs proved to have positive effect on the mechanical properties. Fatigue fracture evaluation of AF reinforced ternary composites showed the positive effect of AFs on fatigue life. AFs reinforced the composites to ensure the integrity of the matrix after a certain number of cycles for the same rubber weight fraction. In addition, increasing rubber content had some favourable effects on the evolution of dynamic secant modulus. Matrix crazing, crack bridging, and shear yielding were determined as toughening mechanisms obtained from SEM observations on fracture surfaces. Considering all the results, these novel composites are green and low-cost solutions for the material manufacturers in automotive and aeronautic industries for the production of various components such as fuel tank mountings and auxiliary parts of suspension system.

ACKNOWLEDGEMENTS

We acknowledge Dr G. Zambelis from Airbus-Helicopter/Paris, France part and also Dr H-A. ALHAS from Airbus-Defence-Space-London-Stevenage/UK who have supported this project. We thank them for their technical help and valuable discussions.

ORCID

Emin Bayraktar https://orcid.org/0000-0003-0644-5249

REFERENCES

1. Adhikari B, De D, Maiti S. Reclamation and recycling of waste rubber. *Prog Polym Sci*. 2000;25(7):909-948.
2. Fiksel J, Bakshi BR, Baral A, Guerra E, DeQuervain B. Comparative life cycle assessment of beneficial applications for scrap tires. *Clean Technol Environ Policy*. 2011;13(1):19-35.
3. De SK, Isayev A, Khait K. *Rubber recycling*. Boca Raton, FL: CRC Press; 2005.
4. Irez AB, Bayraktar E, Miskioglu I. Recycled and devulcanized rubber modified epoxy-based composites reinforced with nanomagnetic iron oxide, Fe3O4. *Compos Part B Eng*. 2018;148:1-13.
5. Lee J, Yee A. Inorganic particle toughening I: micro-mechanical deformations in the fracture of glass bead filled epoxies. *Polymer*. 2001;42(2):577-588.
6. Irez A, Bayraktar E, Miskioglu I. Mechanical characterization of epoxy–scrap rubber based composites reinforced with alumina fibers. In: *Mechanics of Composite and Multi-functional Materials*. Vol.6 Springer; 2018:59-70.
7. Dhingra AK, Peacock N, Ubbelohde AR, Manfre C. Alumina Fibre FP [and Discussion]. *Philos Trans R Soc A Math Phys Eng Sci*. 1980;294(1411):411-417.
8. Wetzel B, Haupert F, Qiu Zhang M. Epoxy nanocomposites with high mechanical and tribological performance. *Compos Sci Technol*. 2003;63(14):2055-2067.
9. Zee RH, Huang YH, Chen JJ, Jang BZ. Properties and processing characteristics of dielectric-filled epoxy resins. *Polym Compos*. 1989;10(4):205-214.
10. Kim J, Kang PH, Nho YC. Positive temperature coefficient behavior of polymer composites having a high melting temperature. *J Appl Polym Sci*. 2004;92(1):394-401.
11. Arayasantiparb D, McKnight S, Libera M. Compositional variation within the epoxy/adherend interphase. *J Adhes Sci Technol*. 2001;15(12):1463-1484.
12. Babbington D, Enos J, Cox J, Barron J. Fast-cure vinyl ester meets automotive structural demands. *Mod Plast Int*. 1987;17(10):106-110.
13. Degrieck J, Van Paepegem W. Fatigue damage modeling of fibre-reinforced composite materials: review. *Appl Mech Rev*. 2001;54(4):279.
14. Wicaksono S, Chai GB. A review of advances in fatigue and life prediction of fiber-reinforced composites. *Proc Inst Mech Eng Part L J Mater Des Appl*. 2013;227:179-195.
15. Sevenois RDB, Van Paepegem W. Fatigue damage modeling techniques for textile composites: review and comparison with unidirectional composite modeling techniques. *Appl Mech Rev*. 2015;67(2):021401.
16. Zhang C, Curiel-Sosa JL, Bui TQ. Meso-scale progressive damage modeling and life prediction of 3D braided composites under fatigue tension loading. *Compos Struct*. 2018;201:62-71.
17. Hu X, Bui TQ, Wang J, et al. A new cohesive crack tip symplectic analytical singular element involving plastic zone length for fatigue crack growth prediction under variable amplitude cyclic loading. *Eur J Mech A Solids*. 2017;65:79-90.
18. Zhang C, Curiel-Sosa JL, Bui TQ. A novel interface constitutive model for prediction of stiffness and strength in 3D braided composites. *Compos Struct*. 2017;163:32-43.
19. Yamamoto N, Guzman de Villoria R, Wardle BL. Electrical and thermal property enhancement of fiber-reinforced polymer laminate composites through controlled implementation of multi-walled carbon nanotubes. *Compos Sci Technol*. 2012;72:2009-2015.
20. Landel RF, Nielsen LE. Mechanical properties of polymers and composites. In: *CRC press*. New York; 1993.
21. Menard KP. *Dynamic mechanical analysis: a practical introduction*. CRC press; 2008.
22. Saba N, Jawaid M, Alothman OY, Paridah MT. A review on dynamic mechanical properties of natural fibre reinforced polymer composites. *Construct Build Mater*. 2016;106:149-159.
23. Wu Y, Chen L, Li J, Zhou H, Zhao H, Chen J. Understanding the mechanical and tribological properties of solution styrene butadiene rubber composites based on partially graphene oxide. *Eur Polym J*. 2017;89:150-161.
24. Gong L-X, Zhao L, Tang L-C, Liu H-Y, Mai Y-W. Balanced electrical, thermal and mechanical properties of epoxy composites filled with chemically reduced graphene oxide and rubber nanoparticles. *Compos Sci Technol*. 2015;121:104-114.
25. Moghaddamzadeh S, Rodrigue D. The effect of polyester recycled tire fibers mixed with ground tire rubber on polyethylene composites. Part II. *Prog Rubber Plast Recycl Technol*. 2018;34(3):128-142.
26. Medina NF, Garcia R, Hajirasouliha I, Pilakoutas K, Guadagnini M, Raffoul S. Composites with recycled rubber aggregates: properties and opportunities in construction. *Construct Build Mater*. 2018;188:884-897.
27. Kalbfleisch JD, Prentice RL. *The Statistical Analysis of Failure Time Data*. 360 Hoboken: J. Wiley; 2011.
28. Hansen U. Damage development in woven fabric composites during tension-tension fatigue. *J Compos Mater*. 1999;33(7):614-639.
29. Catangiu A, Dumitrescu A, Ungureanu D. Experimental results for bending fatigue behaviour of glass-epoxy composite materials. Scientific Bull Valahia Univ, Mater Mech 2011;6:47–51.
30. Beyene AT, Belingardi G, Koricho EG. Effect of notch on quasi-static and fatigue flexural performance of twill E-glass/epoxy composite. *Compos Struct*. 2016;153:825-842.
31. Vallons K, Zong M, Lomov SV, Verpoest I. Carbon composites based on multi-axial multi-ply stitched preforms—part 6. Fatigue behaviour at low loads: stiffness degradation and damage development. *Compos Part A Appl Sci Manuf*. 2007;38(7):1633-1645.
32. Liang S, Gning PB, Guillaumat L. A comparative study of fatigue behaviour of flax/epoxy and glass/epoxy composites. *Compos Sci Technol*. 2012;72(5):535-543.

33. Albouy W. De la contribution de la visco-élasto-plasticité au comportement en fatigue de composites à matrice thermoplastique et thermodurcissable, (Doctoral dissertation) Rouen, INSA; 2013.
34. Montesano J, Selezneva M, Fawaz Z, Poon C, Behdinan K. Elevated temperature off-axis fatigue behavior of an eight-harness satin woven carbon-fiber/bismaleimide laminate. *Compos Part A Appl Sci Manuf*. 2012;43(9):1454-1466.
35. Petermann J. *A Contribution to Evaluate and Predict the Strength and Life Time of Angle-Ply CFRP Laminates Under Static and Cyclic Loads*. Göttingen: Cuvillier; 2004.
36. Ladani RB, Wu S, Kinloch AJ, et al. Improving the toughness and electrical conductivity of epoxy nanocomposites by using aligned carbon nanofibres. *Compos Sci Technol*. 2015;117:146-158.
37. Gong Y, Zhao L, Zhang J, Hu N. An improved power law criterion for the delamination propagation with the effect of large-scale fiber bridging in composite multidirectional laminates. *Compos Struct*. 2018;184:961-968.
38. Ravindran AR, Ladani RB, Wu S, Kinloch AJ, Wang CH, Mouritz AP. Multi-scale toughening of epoxy composites via electric field alignment of carbon nanofibres and short carbon fibres. *Compos Sci Technol*. 2018;167:115-125.
39. Srivastava V, Verma A. Mechanical behaviour of copper and aluminium particles reinforced epoxy resin composites. *Am J Mater Sci*. 2015;5(4):84-89.
40. Zewde B, Pitliya P, Karim A, Raghavan D. Synergistic effect of functionalized carbon nanotubes and micron-sized rubber particles on the mechanical properties of epoxy resin. *Macromol Mater Eng*. 2016;301(5):542-548.
41. Low I-M, Mai Y-W, Bandyopadhayay S. Effects of temperature and rate on fracture toughness of short-alumina-fibre-reinforced epoxies. *Compos Sci Technol*. 1992;43(1):3-12.
42. Kinloch AJ, Young RJ. Shear yielding. In: *Fracture Behaviour of Polymers*. Dordrecht: Springer Netherlands; 1995:107-146.
43. Manjunatha CM, Taylor AC, Kinloch AJ, Sprenger S. The cyclic-fatigue behaviour of an epoxy polymer modified with micron-rubber and nano-silica particles. *J Mater Sci*. 2009;44(16):4487-4490.
44. Huang Y, Kinloch AJ. The role of plastic void growth in the fracture of rubber-toughened epoxy polymers. *J Mater Sci Lett*. 1992;11(8):484-487.
45. Williams JG. Particle toughening of polymers by plastic void growth. *Compos Sci Technol*. 2010;70(6):885-891.
46. Johnsen B, Kinloch A, Mohammed R, Taylor A, Sprenger S. Toughening mechanisms of nanoparticle-modified epoxy polymers. *Polymer*. 2007;48(2):530-541.
47. Blackman BRK, Kinloch AJ, Sohn Lee J, et al. The fracture and fatigue behaviour of nano-modified epoxy polymers. *J Mater Sci*. 2007;42(16):7049-7051.
48. Zotti A, Zuppolini S, Zarrelli M, Borriello A. Fracture toughening mechanisms in epoxy adhesives. In: *Adhesives - Applications and Properties*. Rijeka, Croatia: InTech; 2016.